School of Pharmaceutical and Food Sciences
University of Antioquia

ORIGINAL ARTICLE
Published 11 August 2023
Doi: https://doi.org/10.17533/udea.vitae.v30n2a351025

Check for updates

Analysis of drying kinetic of brewer´s spent grains: effect of the temperature on the physical properties and the content of bioactive compounds

Análisis de la cinética de secado del bagazo residual de malta: efecto de la temperatura sobre las propiedades físicas y el contenido de compuestos bioactivos

E. Gomez-Delgado[1,2,3*], C. Medina-Jaramillo[2], A. Lopez-Cordoba[2]

JOURNAL VITAE
School of Pharmaceutical and Food Sciences
ISSN 0121-4004 | ISSNe 2145-2660
University of Antioquia
Medellin, Colombia

Filliations

[1]Instituto de Tecnología de Alimentos y Procesos Químicos ITAPROQ CONICET. Universidad de Buenos Aires, Facultad de Ciencias Exactas y Naturales, Departamento de Industrias. Int. Güiraldes 2620, Ciudad Universitaria. (C1428BGA) Buenos Aires, Argentina.

[2] Grupo de Investigación en Bioeconomía y Sostenibilidad Agroalimentaria, Escuela de Administración de Empresas Agropecuarias, Facultad Seccional Duitama, Universidad Pedagógica y Tecnológica de Colombia, Carrera 18 con Calle 22, Duitama 150461, Colombia

[3]Grupo de investigación INVEAGRO, Compañía Magia Artesanal S.A.S. Calle 23 A 58 40 T 5AP, Huila, Colombia. * Tel. (+57) -3132211310. E-mail: edwgd@di.fcen.uba.ar, alex.lopez01@uptc.edu.co

***Corresponding**
Edward Gomez-Delgado
edwgd@di.fcen.uba.ar

Received: 25 August 2022
Accepted: 16 July 2023
Published: 11 August 2023

ABSTRACT

Background: Brewer´s spent grain (BSG) is a biomass by-product generated in large volumes during industrial beer production. BSG has become a growing environmental problem, as most breweries discard it inappropriately, negatively impacting the environment. Alternatives for the exploitation of this by-product have consisted of elaborating food supplements for farm animals, obtaining biofuels, developing adsorbents, and obtaining substances for the food industry. However, the high moisture content in BSG (approximately 70%), poses a significant challenge in exploring various reuse alternatives. Therefore, the implementation of a pre-drying process becomes essential. **Objective:** This study aimed to analyze the BSG drying kinetics at different temperatures and the effect of the drying temperature on the physical properties and the content of bioactive compounds. **Methods:** BSG samples were dried at different temperatures (50, 60, 70, 80, 90, and 105°C) and analyzed for their moisture ratio, water activity, total polyphenol content (TPC), and DPPH (1,1-diphenyl-2-picrylhydrazil) radical scavenging activity. Also, four kinetics models were fitted to the drying data. **Results:** It was determined that the effective diffusivity was between 5.23×10^{-10} (m^2/s) and 2.49×10^{-09} (m^2/s), and the value of the activation energy was 28.05 kJ/mol. In addition, it was found that the content of phenolic compounds (1.27±0.120 mg gallic acid equivalents /g) and the DPPH radical scavenging activity (0.21±0.015 mg gallic acid equivalents /g) were not significantly affected by the variation in the drying temperatures studied. **Conclusions:** From an operational point of view, the most suitable temperature for the drying process of BSG was 105°C since it would allow to reach shorter drying times, and the TPC was not affected markedly by the range of temperature studied.

Keywords: *Brewer´s spent grain, dry kinetics, diffusion, polyphenols, by-products valorization.*

RESUMEN

Antecedentes: El Bagazo residual de malta (BSG por sus siglas en inglés) es un subproducto biomásico generado en grandes volúmenes durante la producción industrial de cerveza. El BSG se ha convertido en un creciente problema para el medio ambiente, debido a que la mayoría de las cervecerías descartan inapropiadamente este residuo generando un impacto negativo al ambiente. Las alternativas para el aprovechamiento de este subproducto han consistido especialmente en la elaboración de suplementos alimenticios para animales de granja, obtención de biocombustibles, desarrollo de adsorbentes y obtención de productos para la industria alimentaria. Sin embargo, el alto contenido de humedad (~70%) del BSG representa un reto para el desarrollo de diferentes alternativas de reutilización, por lo que se hace necesario un proceso de secado previo. **Objetivos:** En este estudio se analizó la cinética de secado del BSG a diferentes temperaturas y el efecto de la temperatura de secado sobre sus propiedades físicas y contenido de compuestos bioactivos. **Métodos:** Las muestras de BSG fueron secadas a diferentes temperaturas (50, 60, 70, 80, 90 y 105°C) y analizadas en términos de razón de humedad, actividad acuosa, contenido de polifenoles totales (TPC) y actividad secuestradora del radical DPPH. Además, se ajustaron 4 modelos cinéticos a los datos de secado. **Resultados:** Se determinó que la difusividad efectiva del BSG varió entre 5.23×10^{-10} (m^2/s) y 2.49×10^{-09} (m^2/s). El valor de la energía de activación fue de 28.05 kJ/mol. Además, se encontró que el contenido de compuestos fenólicos (1.27±0.120 mg equivalentes de ácido gálico/g) y la actividad secuestradora del radical DPPH (0.21±0.015 mg equivalentes de ácido gálico/g) no se vieron significativamente afectados por el rango de temperaturas estudiadas. **Conclusiones:** Desde un punto de vista operativo, se determinó que la temperatura de secado más adecuada para el BSG fue de 105°C, debido a que permitió alcanzar tiempos de secado más cortos, y además, el TPC no se vio significativamente afectado en el rango de temperaturas estudiadas.

Keywords: *Bagazo residual de malta, cinética de secado, diffusion, polifenoles, valorización de subproductos.*

INTRODUCTION

Within the alcohol industry, beer is the most consumed drink globally (1,2). Over time, the brewing process has undergone various transformations until it reaches the industrial production process that we generally know today (1,3,4). The process of obtaining the beer consists of the malting stage of the fermentable source (barley grain, rice grain, among others), grinding and maceration, obtaining the wort, refrigeration, and fermentation (5). A solid and wet by-product is obtained during maceration, known as Brewer´s spent grain (BSG). BSG represents 85% of all solid by-products generated by beer production (4,6).

World beer production for 2018 reached ~1940×10^6 hectolitres (194×10^6 m^3) (6), of which ~582×10^6 hectolitres (~30% of world production) were produced in the Americas (7). The countries with the highest beer production for 2020 were China (~341×10^6 hectolitres), the USA (~212×10^6 hectolitres), and Brazil (~152×10^6 hectolitres) (8). In Colombia, it is estimated that the annual production of beer is approximately 22×10^6 hectolitres (8), considering that for every 100 liters of beer obtained, 20 kg of BSG are produced (6), the amount of bagasse generated is a little over 440×10^3 Ton per year. These large volumes of by-products are becoming a growing environmental problem due to their unwillingness to discard them (4,6,7,9–11).

In recent years there has been growing scientific and political interest in the exploitation and valorization of residual biomass (12), such as BSG. It is partly due to the concept of circular bioeconomy has gained in the global economy (13,14). The circular bioeconomy consists of an environmentally and socially sustainable economy through biological resources production, use and reuse (15,16). Therefore, finding different alternatives for using residual biomass, such as BSG, is considered a current challenge for scientific research.

Searching for technological alternatives for the use of BSG has brought with it the development and application of different technologies, for example, a food supplement for farm animals based on BSG due to its rich protein content (17). Other studies have found that it can be used for energy production (18), obtaining biodiesel (19), and bioethanol (20). Other authors have investigated the use of BSG for various purposes, such as obtaining coenzymes, graphene for electrode production (21), activated carbons (22), and obtaining food products for human consumption (23), among others.

The BSG has a high moisture content (~70-73%) (19,24,25); this makes it challenging to handle and store. In addition, higher moisture favors the presence of microorganisms that degrade biomass making it difficult to reuse and practical application for the options mentioned above. In line with reusing the BSG, it must be made a pre-drying treatment to improve its handling and storage conditions. Various drying techniques have been employed, including infrared, freeze drying, convective hot air drying, and solar drying. Among these methods, convective drying is the widely utilized approach in industrial settings for mass production (26–30). During the development of a laboratory-scale production process, it is crucial to consider upscaling it for industrial applications. Therefore, gaining a comprehensive understanding of drying kinetics becomes paramount, with theoretical and semi-theoretical models playing a pivotal role in this regard.

Semi-theoretical models are typically derived by simplifying the general series of Fick's second law or modifying existing simplified models (31). Empirical and semi-theoretical models have the advantage of requiring less computational time and do not necessitate complex assumptions about the geometry, mass diffusivity, and conductivity of the specific food product (31). These models have been widely used for modeling the drying kinetics of agri-food products such as watermelon seeds, turnips, and coffee beans (26,29,32,33). In the literature, few kinetic studies of BSG drying are directed to find the best drying temperature and its influence on some characteristics such as water activity, intrinsic moisture of BSG drying, and the content of antioxidant compounds present in the extract obtained.

This work aimed to study a temperature range for the drying process of the BSG, favoring the operation time. For this purpose, drying kinetics were studied, and different kinetic models were applied to the experimental data to predict drying behavior. Fick's second law of mass transfer was used to determine effective diffusivity and activation energy. The change in moisture ratio, water activity, and color of the BSG after drying at different temperatures was also evaluated. Finally, the influence of the drying temperature on the content of phenolic compounds and the antioxidant activity of the BSG was evaluated.

2. MATERIALS AND METHODS

2.1. Materials

Brewer´s spent grain (BSG) was supplied by a brewing company in the tatacoa desert (Huila, Colombia). The bagasse was frozen for storage and later use. Ethanol (70% v/v) and analytical grade sodium carbonate (Na_2CO_3) (LOBA Chemie, India) were used. Folin-Ciocalteu reagent, gallic acid, and the 1,1-diphenyl-2-picrylhydrazil (DPPH) free radical were purchased from PanReac ApliChem (Spain).

2.2. Drying assays

The drying process of the BSG was carried out on a convection oven (Memert UF 110, Memmert Universal, Schwabach, Germany) equipped with a temperature controller. The evaluated temperatures (50°C, 60°C, 70°C, 80°C, 90°C, and 105°C) were selected based on previous studies and practical considerations, aiming to cover a wide range of drying conditions commonly encountered in industrial and laboratory settings (26,29,33). The process consisted of weighing approximately 10 g of BSG in a Petri box, putting it into the oven, and drying it at the defined temperature. The variation in the sample weight was recorded at intervals; this procedure was repeated until constant weight, indicating that the equilibrium had been reached. The weight recorded up to equilibrium also allowed the sample to obtain moisture. Under the established conditions, it was assumed that the resistance to heat transfer within the particle and in the outer gaseous phase was negligible (33). The reported results corresponded to average values obtained from tests performed in triplicate at each temperature.

The moisture ratio was (MR) obtained by applying the following equation (Eq 1) (34):

$$MR = \frac{m_t - m_e}{m_i - m_e} \tag{1}$$

where m_t is the moisture content at time t, present in the BSG; m_i is the initial moisture content of the sample, and m_e is the moisture at the equilibrium over a long enough time to ensure constant weight. Four commonly used mathematical models were used to adjust the drying curve under isothermal conditions (31): Newton, Page, Logarithmic, and Midilli-Kucuk. The differences between the experimental and theoretical values given by each model were evaluated using the statistics of the adjusted coefficient of determination (R^2_a), the standard deviation (SD), and the coefficient of variance (CV).

$$R^2{}_a = 1 - \left[\frac{N-1}{N-p-1} * \left(1 - R^2\right) \right] \tag{2}$$

$$SD = \frac{\sqrt{\sum_{i=1}^{N} \left(MR_{exp} - MR_{mod} \right)^2}}{N-1} \tag{3}$$

$$CV = \frac{SD}{\overline{MR_{exp}}} \tag{4}$$

where N is the number of experimental data; p is the number of model parameters; R^2 is the coefficient of determination; MR_{exp} is the experimental moisture data; MR_{mod} is the theoretical moisture, and $\overline{MR_{exp}}$ is the average of the experimental moisture data.

2.3. Determination of the effective diffusivity

The equation of the second law of Fick Eq (5) was used for effective diffusivity (D_{eff}) determination. This equation describes the diffusion of water during the drying process, where the resistance to mass transfer that limits the drying speed is given by internal resistance, that is, the transfer of water from inside the BSG to the surface (35,36).

$$\frac{\partial MR}{\partial t} = \nabla\left[D_{eff}\left(\nabla MR\right)\right] \tag{5}$$

One of the analytical solutions of the second law of Fick for flat geometries, long drying periods and values of $MR<0.6$ is presented in Eq (6) (37).

$$MR = \frac{8}{\pi^2} - \exp\left(\frac{\pi^2\ D_{eff}}{L^2}\ t\right) \tag{6}$$

where D_{eff} is the effective diffusivity (m^2/s), L is the characteristic length (m), and t is the drying time (s). Characteristic length L was determined using Eq. (7), considering the mass of the sample W, the density ρ, and the cross-sectional area of the sample A_t.

$$L = \frac{W}{\rho\, A_t} \tag{7}$$

It is known that effective diffusivity can commonly be determined by graphing the experimental data linearizing Eq. (6) as shown in Eq (8).

$$\ln\left(\ddot{u}\quad\right) = \ln\frac{8}{\pi^2} - \left(\frac{\pi^2\ D_{\ddot{u}}}{L^2}\right) \tag{8}$$

After plotting ln(MR) vs. t, the D_{eff} value was obtained from the slope of equation Ec (8). For calculating the activation energy E_o an expression of Arrhenius was used (19,34) Eq. (9), which relates effective diffusivity, temperature, and activation energy. Where D_o is the pre-exponential factor; T is the absolute temperature; and R is the general constant of the gases.

$$D_{eff} = D_o\, exp^{\left(\frac{-E_o}{R\,T}\right)} \tag{9}$$

2.4 Moisture and water activity.

For intrinsic moisture determination, approximately 0.5g of dry and ground BSG was weighed in a moisture balance (Citizen MB-50 Moisture Analyser Balance, Japón). The water activity was determined in a water activity analyzer equipment (AquaLab PRE, USA), the sample was entered, and the value determined by the equipment was recorded. All measurements were made in triplicate for each BSG sample dried at the studied temperatures. The recorded value corresponds to the average value of the measurements.

2.5 Color

The color of the dry samples was measured using a tristimulus Minolta colorimeter (Konica-Minolta CR-10, Osaka, Japan) and reported in CIELab parameters (L*, a* and b* values), where L* was used to denote lightness, a* redness and greenness, and b* yellowness and blueness (38). The equipment was calibrated using a white plate as standard. BSG samples were placed on this white plate, and the values of the parameter's "L", "a" and "b" were recorded. The total color difference (ΔE) was calculated using equation Eq (10).

$$\Delta E = \sqrt{\left(L - L^{\ddot{u}}\right)^{\ddot{u}} + \left(a - a\ \right) + \left(b - b\ \right)} \tag{10}$$

2.6 Determination of the content of bioactive compounds

Samples (1 g) of BSG were placed in 15 mL test tubes and mixed with 6 mL of 70 %v/v ethanol. Then, the tubes were immersed in an ultrasound bath (BRANSON model 1800, Germany) with a rectangular chamber (longe:10 cm, hight:12 cm, depth: 12 cm) equipped with an industrial transducer operating at 40 kHz. A flow system (in/out) controlled the water temperature from a heating bath (Memmert WNB14, Germany), maintaining a constant temperature of 60 °C for 10 minutes. The extracts obtained were filtered (Double ring qualitative filter paper, grade: EXP DRQLM) and centrifuged at 5300 m/s^2 (4000 rpm) for 10 min. The extracts were suspended in water for all determinations at a dilution factor of 9. This test was carried out in triplicate for each dried BSG sample at the studied temperatures.

2.6.1 Estimation of total polyphenols content

The total polyphenols content (TPC) of BSG was determined by the Folin-Ciocalteu method (39).

Briefly, 400 µL of each extract were mixed with 2 mL of 1:10 diluted Folin-Ciocalteu reagent. The mixtures were stirred for 30 s using a vortex mixer (Benchmark, USA), and then 160 µL of sodium carbonate (7% w/v) were added. After 30 min, the absorbance of the samples was measured at 760 nm using a spectrophotometer (X-ma 1200 Human Corporation, Loughborough, UK). Gallic acid was used as standard. The total polyphenols content was expressed as gallic acid equivalents (GAE) per gram of BSG.

2.6.2 Estimation of the DPPH•–scavenging activity

DPPH radical scavenging activity was tested as described Brand-Williams *et al.* (1995) (40). A volume of 100 µL of each obtained extract was mixed with 3,9 mL of an ethanolic solution of DPPH• (25 ppm). It was then vortexed for 30 s and kept in the dark for 30 min. Finally, the absorbance was measured at 517 nm using the spectrophotometer. Gallic acid was also used as standard, and the results were expressed as mg gallic acid per gram BSG (mg GAE/g BSG).

3. RESULTS AND DISCUSSIONS

3.1. Drying kinetics analysis

Figure 1 shows the drying curves of Brewer´s spent grain (BSG) obtained at the different studied temperatures (50°C, 60°C, 70°C, 80°C, 90°C, and 105°C). It was observed that when the temperature increases, the curve's slope becomes greater, indicating that the humidity of the BSG reaches equilibrium or reaches a specific moisture ratio in shorter times. The equilibrium time is defined as the moment when sample mass does not vary in time; according to this, for the dried sample at 105°C, the equilibrium time was reached at 60 min, while at 50 °C, the equilibrium time took 260 min, four times more than observed at 105 °C. Recent studies on the drying kinetics of biomass corroborate the influence of temperature on the drying process. For instance, Ghanem et. al. found that increasing the drying temperature from 50 to 70 °C reduced the drying time by 30 % (41). Similarly, another study reported that temperature is a critical factor for the drying kinetics of sawdust, affecting the drying process (42). Additionally, the literature suggests that the drying kinetics of biomass are affected by various parameters, including the type and size of biomass, airflow rate, and moisture ratio. For example, a study by (43) examined the drying kinetics of palm kernel shells and determined that airflow rate and particle size significantly affect the drying process. From these curves presented in Figure 1, it was also determined that the initial humidity of BSG was 71.7 % (±0.012). This moisture ratio aligns with others reported in the literature (37,44).

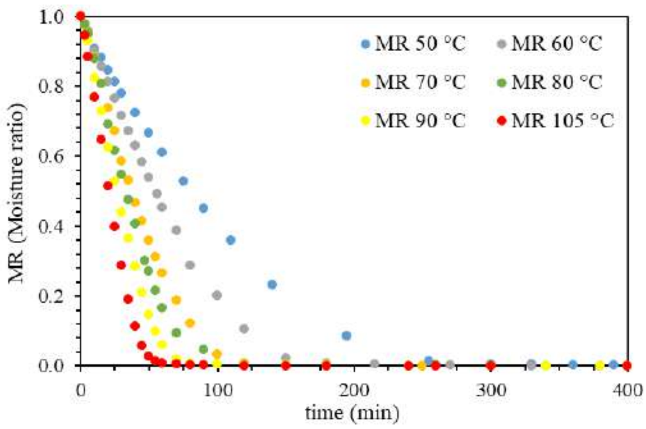

Figure 1. Drying curves of Brewer´s spent grain (BSG) using the different temperatures studied (experimental points).

The drying speed curves of BSG obtained at the different studied temperatures are shown in Figure 2. It was observed that as the temperature increased, the slope of the curve was higher, indicating an increase in the drying speed. Besides, at the beginning of the curve, the positive slope indicated a short period where the drying speed increased. This increase corresponded to the period when the temperature inside the oven raised, promoting the evaporation process of the water from the particles' surface. It should be noted that this period became shorter as the temperature studied increased. Similar observation has been reported in previous studies on the effect of temperature on the drying rate of biomass (45). A progressive decay of the drying rate was observed because the moisture on the surface of the particles was completely evaporated, while the remaining water within the BSG matrix evaporated slower. This behavior indicated that the internal resistance limits the drying speed to mass transfer, that is the diffusion of moisture from inside the BSG to its surface. Similar drying mechanism have been observed in other studies (19, 31, 33, 37, 46). These findings were consistent whit other studies on the drying kinetics of bamboo sawdust reported, the drying rate augmented with increasing temperature, and the drying process can be divided into three stages: the initial increasing rate period, the constant rate period, and the falling rate period, which was consistent with the observations made in this (47, 48).

Figures 1 and 2 show that the drying speed was not constant in any of the conditions studied, probably because the thickness of the moisture layer, the "thin layer" on the surface, was not constant, preventing a continuous supply of moisture during the drying process. This behavior has also been observed in other studies (31, 46, 48).

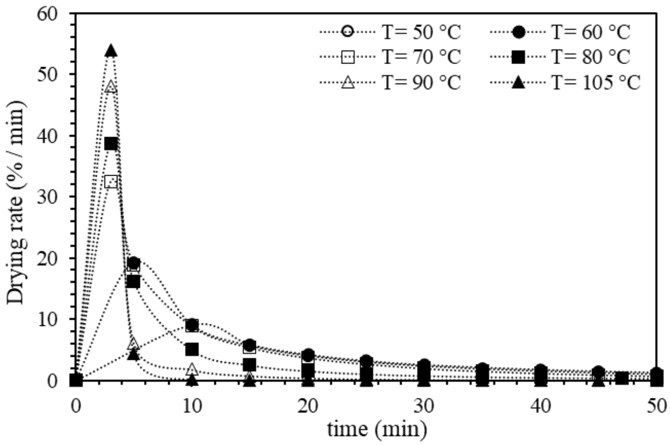

Figure 2. Drying speed curves of Brewer´s spent grain (BSG) at the different temperatures studied.

The BSG drying curve was also evaluated using different masses; for this purpose, 105°C was used as the drying temperature because the process was performed faster. Figure S1 describes the drying curves at 105°C using different masses of BSG; it can be seen that the slope of the curve increased as the mass of BSG to be dried decreased. Also, the humidity to reach balance took 50, 60, and 80 min for 5g, 10g, and 15g, respectively. Therefore, the drying process took longer when there was more bagasse mass. This result corroborated that the internal resistance to mass transfer by the diffusion of moisture from the inside BSG particle to its surface was the limiting drying speed, as mentioned above, which is a common limiting factor in the drying kinetics of biomass. However, it is important to note that the drying kinetics of diverse types of biomasses may be influenced by various factors such as temperature, relative humidity, and particle size (30, 47, 48). Therefore, a comprehensive understanding of the drying behavior of each type of biomass is necessary to optimize the drying process for industrial applications.

3.2. Analysis of the effective diffusivity and of the activation energy of the drying process.

Assuming that the sample throughout the drying process presented a negligible shrinkage, uniform distribution, and a constant content of initial moisture throughout the BSG particle, one of Fick's second law solutions was used to determine effective diffusivity. Figure S2 shows the graphs of Ln (moisture ratio (MR)) vs. t (min), using equation Eq (8) and using the slope of each line was determined the effective diffusivity in each temperature studied.

Table 1 shows the values of effective diffusivity at different temperatures. Since D_{eff} was influenced by temperature, pressure, and molecular weight, the pressure, and molecular weight was assigned a constant value for this drying study. The increasing temperature and the effective diffusivity were greater because the higher the temperature increased the energy necessary for the water particles to begin the diffusion through the internal structure of the BSG (Table 1). D_{eff} values in this analysis were in the order of magnitude found for other biomasses studies using BSG (33, 37). However, other recent studies have reported different results. For example, a study on the drying kinetics of corn stover reported that the effective diffusivity decreased with increasing temperature due to the formation of a crust layer on the biomass surface, which hindered moisture transfer (49, 50). These discrepancies highlight the importance of studying the specific characteristics of each type of biomass and the potential formation of crust layers during the drying process, as well as the need for further research to optimize drying conditions and reduce energy consumption in biomass drying processes.

Table 1. Effective diffusivity at different temperatures and constant pressure (101.325 kPa)

Temperature (°C)	50	60	70	80	90	105
Effective diffusivity (m^2/s)	5.23×10^{-10}	8.22×10^{-10}	1.29×10^{-09}	1.39×10^{-09}	1.91×10^{-09}	2.49×10^{-09}

For the biomass drying process, such as BSG, the activation energy can be defined as the energy necessary for water particles to begin to diffuse through the solid structure of the BSG to the surface, and the drying process occurs (32, 51). For Activation Energy determination *Eo* (kJ/mol), the *Deff* values recorded at the different temperatures were used; for this purpose, the Ln (*Deff*) vs. 1/T was plotted (Figure S3). The results showed *Eo* values of around 28.05 kJ/mol. The pre-exponential coefficient D_o with a value of 2.04x10^{-5} m^2/s was also determined. Activation energy has been widely used to analyze the drying kinetics of various types of biomasses, such as stevia leaves (52), tea (53), fructus aurantii (dried fruit of *Citrus aurantium* L.) (54), pomegranate arils (55), wood (56). These studies have reported activation energy values ranging from 13.5 kJ/mol for tea to 41.5 kJ/mol for wood, indicating that different types of biomasses have different activation energies due to variations in their internal structure and composition. In contrast, the *Eo* value obtained in this study for BSG was 28.05 kJ/mol, which is relatively low compared to other biomass studies. This difference in *Eo* values between BSG and other biomass is due to the unique structure and composition of BSG.

3.3. Analysis of the kinetic models

For kinetics analysis, four mathematical models were used to fit the experimental data: the model of Newton, Page, Logarithmic, and Midilli-Kucuk. With these models, it was desired to obtain the most suitable equation to estimate the moisture ratio (MR) of bagasse drying at different temperatures. Kinetic models are represented by the following Eq. (11-14):

Newton model $: MR = exp\left(-Kt\right)$ (11)

Page model $: MR = exp\left(-Kt^n\right)$ (12)

Logarithmic model $: MR = a + b\,exp\left(-Kt\right)$ (13)

Midilli-Kucuk model $: MR = a\,exp\left(-Kt^n\right) + bt$ (14)

where *K* is the kinetic constant of each model, n is a power constant, a and b are parameters of the corresponding equation.

Figures 3 and 4 show the different models adjusted to the experimental data to facilitate the graphical analysis. The figures were grouped between the best-adjusted models (Figure 3) and those with more significant deviation (Figure 4).

Figure 3 shows the kinetic models that best fit the experimental data, the Page and Midilli-Kucuk models. In part, this is because the Midilli-Kucuk model contains a greater number of parameters with respect to the Page model; it was found that an equation with two parameters allows to adequately describe the drying kinetics of the BSG, in addition to being used to estimate the moisture ratio. Figure 4 shows the two kinetic models that had greater deviation when adjusting to the experimental data, Newton and the Logarithmic; observing that despite not adjusting as well as the Page and Midilli-Kucuk models, they could be used cautiously to have an estimated value of moisture during the drying process.

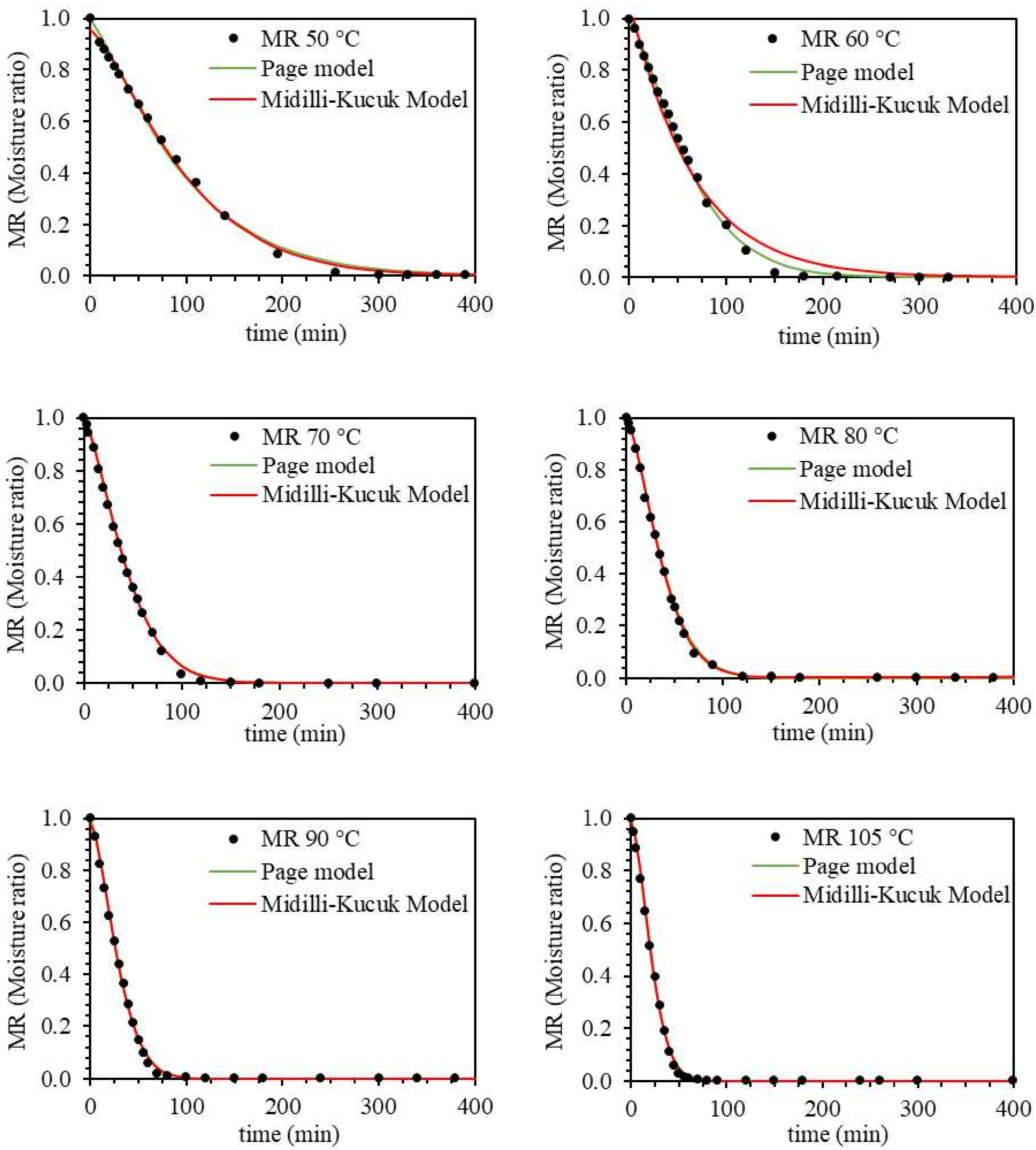

Figure 3. Page and Midilli-Kucuk kinetic models adjusted to experimental drying curve data at different temperatures (50 °C, 60 °C, 70 °C, 80 °C, 90 °C, and 105 °C).

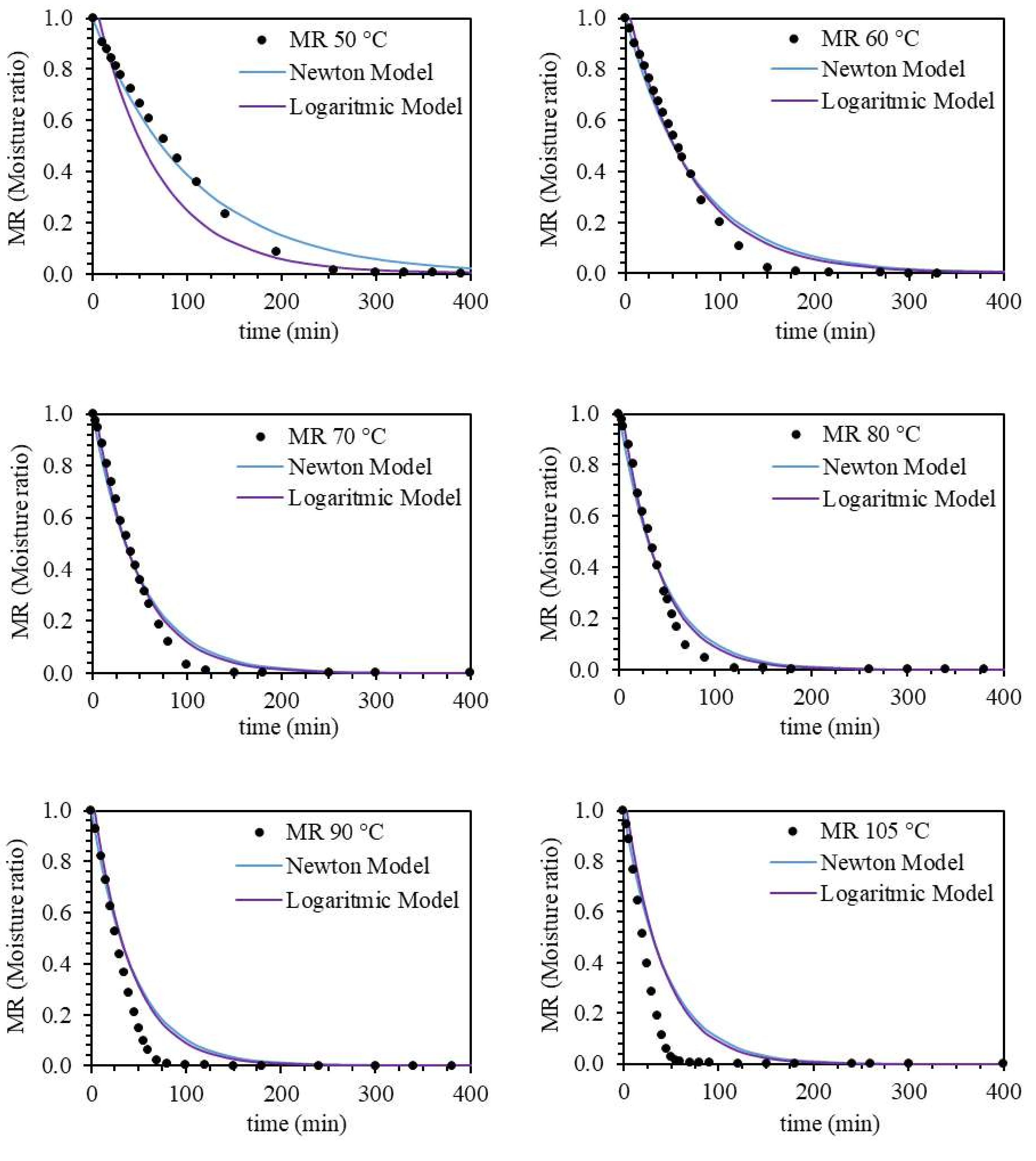

Figure 4. Newton and logarithmic kinetic models adjusted to experimental drying curve data at different temperatures (50 °C, 60 °C, 70 °C, 80 °C, 90 °C, and 105 °C).

Table 2 presents the parameters of the different kinetic models adjusted to the experimental data. All parameter values from the kinetic models used are in the order of those found in the literature (29, 33, 51). The Page model was the one that best fit the experimental data; this can be deduced because this model obtained the values of R^2 higher, lower *SD*, lower *CV*, and better graphic fit (Figure 3, Table 2). This model contains relevant information to drying kinetics from the two parameters that fit the

Page equation. The kinetic constant K and n grew slightly as the drying temperature increased. The growth of K was in line with the above results; as the temperature increased, the slope became larger. From the above, we concluded that a kinetic model with two parameters was sufficient to describe the drying kinetics of BSG adequately. The Page model allowed to have a robust model for predicting the drying kinetics of the precursor without the need to use a more complex equation using a greater number of parameters.

Table 2. Kinetics models parameters

Model	Temperature	Parameters				Statistics		
	(°C)	a	B	n	K (s^n)	r^2	*SD*	*CV*
Newton	50	-	-	-	0.0094	0.9897	0.038	0.085
	60	-	-	-	0.0137	0.9791	0.050	0.110
	70	-	-	-	0.0201	0.9724	0.055	0.112
	80	-	-	-	0.0229	0.9710	0.060	0.142
	90	-	-	-	0.0229	0.8964	0.108	0.344
	105	-	-	-	0.0229	0.7347	0.065	0.222
Page	50	-	-	1.2024	0.0038	0.9968	0.021	0.046
	60	-	-	1.3462	0.0033	0.9976	0.016	0.036
	70	-	-	1.3870	0.0046	0.9985	0.012	0.025
	80	-	-	1.4586	0.0042	0.9983	0.014	0.033
	90	-	-	1.5158	0.0049	0.9978	0.015	0.048
	105	-	-	1.5728	0.0063	0.9975	0.017	0.057
Logarítmico	50	1.00E-03	1.1000	-	0.0150	0.9281	0.095	0.213
	60	3.00E-07	1.0687	-	0.0150	0.9838	0.042	0.092
	70	6.00E-07	1.0721	-	0.0219	0.9792	0.045	0.091
	80	3.00E-07	1.0863	-	0.0252	0.9774	0.048	0.114
	90	6.00E-07	1.0863	-	0.0252	0.8906	0.102	0.326
	105	5.00E-07	1.0863	-	0.0252	0.6951	0.056	0.190
Midilli-Kucuk	50	0.9583	0.00E+00	1.3223	0.0021	0.9976	0.016	0.036
	60	1.0691	5.00E-07	1.0246	0.0137	0.9847	0.039	0.087
	70	0.9863	6.00E-07	1.4262	0.0039	0.9985	0.011	0.023
	80	0.9934	6.00E-06	1.5006	0.0037	0.9990	0.010	0.023
	90	0.9786	4.00E-07	1.5753	0.0039	0.9978	0.014	0.044
	105	0.9711	5.00E-07	1.6678	0.0044	0.9979	0.014	0.048

Figure S4 shows the kinetic models adjusted to the drying curves at a temperature of 105 °C using different masses of BSG. The parameters of the kinetic models were reported in Table S1. From Figure S4 and Table S1, the Page and Midilli-Kucuk models presented the best adjustments to the experimental data. In contrast, the Newton and Logarithmic models presented the greatest deviation. This behavior was similar to those illustrated in Figures 3 and 4.

3.4. Analysis of moisture and water activity

The effect of drying temperature on moisture content, water activity, and color of BSG after drying was analyzed. In addition, it was explored whether the BSG milling process affected the characteristics mentioned above after the drying process. These characteristics were compared in dry and whole BSG with dry and ground BSG.

Figure 5 shows the behavior of the water activity (a_w) and the moisture of BSG as a function of the drying temperature. It was observed that the moisture and the water activity of BSG did not vary significantly, regardless of the temperature used in the drying. Besides, the whole and ground BSG samples showed moisture values of around 4.8% (±1.614) and 4.0% (±0.366), respectively, while similar a_w values were obtained for both samples (a_w~0.26-0.28) (Figure 5a). This result is an advantage from an application point of view since a material with low water activity and low moisture could stay longer in storage without affecting its shelf life, reducing the deterioration risk of BSG.

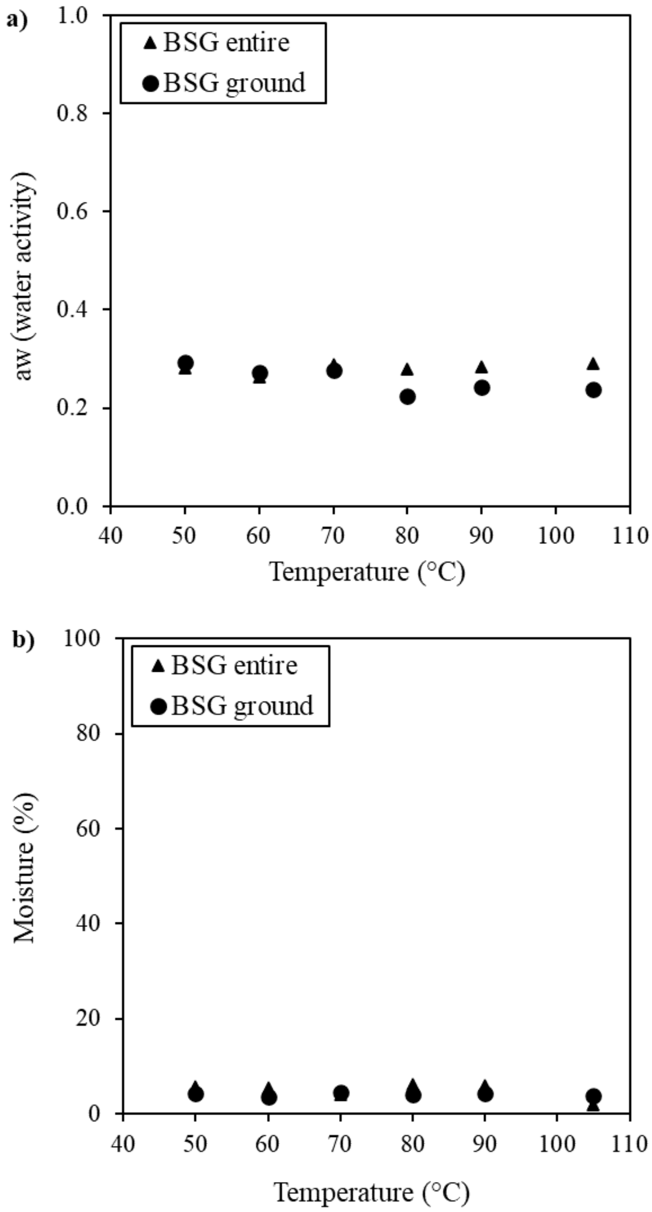

Figure 5. Behavior of the water activity (a), and the moisture content (b) of the BSG samples as a function of drying temperature. These properties were measured for entire BSG and ground BSG.

3.5. Color

Figure S5 shows images of the whole and ground BSG samples, while the corresponding Δ*E* values are shown in Table S2. It was observed that the different temperatures studied did not cause significant changes in the appearance of the samples nor in their color attributes. This behavior was probably due to the relatively low temperatures used, which were insufficient to alter the pigments present in both whole and ground BSG. Some studies reported that high drying temperatures can lead to a decrease in brightness and chroma of biomass samples, indicating a color change (53, 54, 57, 58). Therefore, it could be suggested that the effect of drying temperature on color stability varies depending on the specific type of biomass and the drying conditions used.

3.6. Analysis of the total phenolic content and DPPH radical scavenging activity

Figure 6 shows the behavior of the total polyphenol content and the DPPH radical scavenging activity of the BSG samples as a function of drying temperature.

The different drying temperature studied did not significantly influence the TPC (Figure 6a) or the DPPH radical scavenging activity (Figure 6b). The average phenolic content and DPPH scavenging activity were 1.27±0.120 mg GAE/g BSG and 0.21±0.015 mg GAE/g BSG, respectively. Yan et al. reported that the drying temperature had an impact on TPC and DPPH radical scavenging activity in both hot-air-dried and sunlight-dried orange black tea. Specifically, an increase in the drying temperature of orange black tea led to a decrease in TPC and antioxidant activity of the extract, with a more pronounced effect when hot-air was used as the drying method (53). Conversely, a previous study on microwave drying of lemon peel demonstrated an increased TPC when the applied power was augmented. This behavior was attributed to the generation of high vapor pressure and temperature inside the plant tissue caused by the intense heat produced by microwaves, leading to the disruption of plant cell wall polymers. As a result, bound or cell wall phenolics may be released, potentially resulting in an increased extraction of phenolic compounds (41).

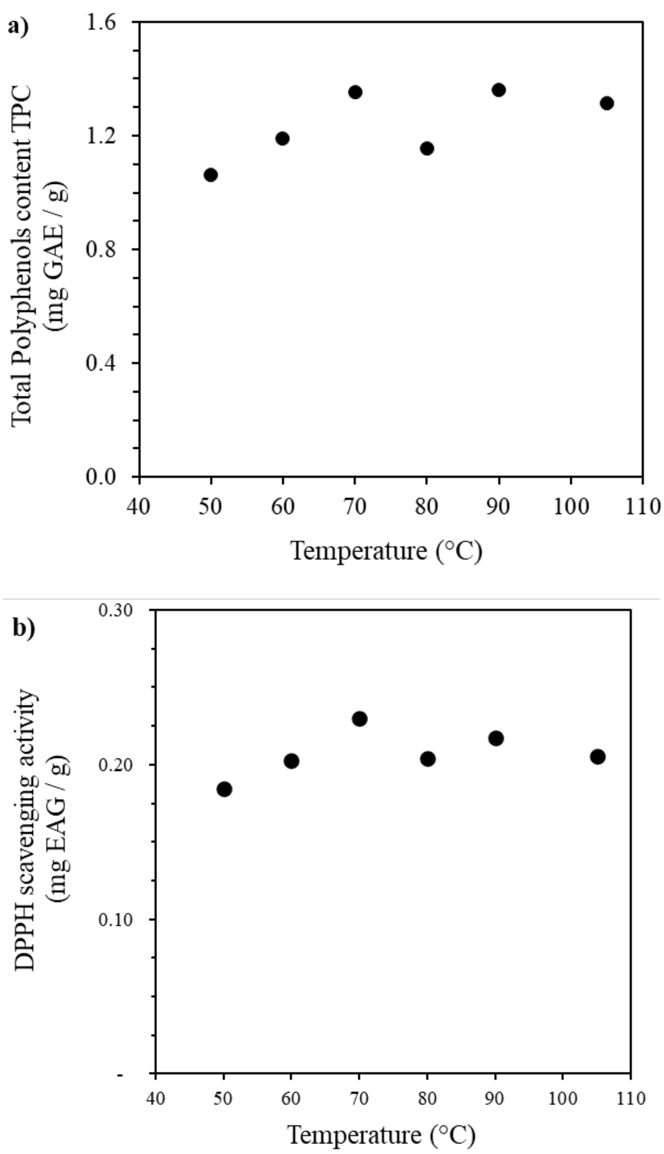

Figure 6. Behavior of the total polyphenols content (a), and the DPPH radical scavenging activity (b) of the BSG samples as a function of drying temperature.

CONCLUSIONS

Drying kinetics of Brewer´s spent grain at different temperatures (50 °C, 60 °C, 70 °C, 80 °C, 90 °C, and 105 °C), and the effect of the drying temperature on the physical properties and the content of bioactive compounds were studied. It was observed that the internal diffusion of moisture limited the drying speed; the internal resistance is the governing mechanism for moisture transfer. The effective diffusivity values determined ranged from 5.23×10^{-10} (m^2/s) to 2.49×10^{-09} (m^2/s), and the activation energy value was 28.05 kJ/mol. The Page and Midilli-Kucuk models showed the best fit for the experimental data. In particular, a kinetic model with two parameters, such as the Page model, was sufficient to adequately describe the drying kinetics of BSG without the need to use a more complex equation using a greater number of parameters. Regardless of the drying temperature, the obtained BSG presented a low water activity and low intrinsic humidity that favors, in principle, greater storage and conservation times. It could be observed that the total phenolic content of 1.27 (±0.120) mg EAG/g BSG and DPPH radical scavenging activity 0.21 (±0.015) mg EAG/g BSG, present in the extract obtained from BSG, was not affected by temperature variation in the studied range. Therefore, phenolic compounds have antioxidant properties and can be used as animal food supplements. From an operational point of view, it is possible to conclude that the most suitable temperature for the drying process of BSG was 105 °C since it allowed shorter drying times. The latter would result in lower energy and operating costs. Studies are recommended to extract polyphenols utilizing Ultrasound-assisted extraction (UAE) on a larger scale (pilot or industrial) to determine the feasibility of reusing BSG as a source of antioxidant substances by evaluating economic aspects, energy, and operations.

Conflicts of Interest: The authors declare no conflict of interest.

Acknowledgement: The authors acknowledge to Universidad Pedagógica y Tecnológica de Colombia (UPTC), Magia Artesanal S.A.S. company and its research group INVEAGRO, Consejo Nacional de Investigaciones Científicas y Técnicas (CONICET) and Universidad de Buenos Aires for financial support.

Author Contributions: Conceptualization was devised by A.L.-C. and C.M.-J; methodology, validation, and formal analyses, investigation, resources, data curation, writing—original draft preparation and writing—review and editing, data visualization was performed by E.G.-D.; project administration and funding acquisition were performed by A.L.-C. All authors have read and agreed to the published version of the manuscript.

REFERENCES

1. Gómez-Corona C, Escalona-Buendía H, García M, Chollet S, Valentin D. Craft vs. industrial: Habits, attitudes and motivations towards beer consumption in Mexico. Appetite. 2016;96:358–67. DOI: https://doi.org/10.1016/j.appet.2015.10.002
2. Villacreces S, Blanco C, Caballero I. Developments and characteristics of craft beer production processes. Food Biosci. 2022;45:101495. DOI: https://doi.org/10.1016/j.fbio.2021.101495
3. Melewar T, Skinner H. Territorial brand management: Beer, authenticity, and sense of place. J Bus Res. 2020;116:680–9. DOI: https://doi.org/10.1016/j.jbusres.2018.03.038

4. Anderson H, Santos I, Hildenbrand Z, Schug K. A review of the analytical methods used for beer ingredient and finished product analysis and quality control. Anal Chim Acta. 2019;1085:1–20. DOI: https://doi.org/10.1016/j.aca.2019.07.061

5. Mussatto S, Dragone G, Roberto I. Brewers' spent grain: Generation, characteristics and potential applications. J Cereal Sci. 2006;43(1):1–14. DOI: https://doi.org/10.1016/j.jcs.2005.06.001

6. Sganzerla W, Ampese L, Mussatto S, Forster-Carneiro T. A bibliometric analysis on potential uses of brewer's spent grains in a biorefinery for the circular economy transition of the beer industry. Biofuels, Bioproducts and Biorefining. 2021;15(6):1965–88. DOI: https://doi.org/10.1002/bbb.2290

7. Wagner E, Pería M, Ortiz G, Rojas N, Ghiringhelli P. Valorization of brewer's spent grain by different strategies of structural destabilization and enzymatic saccharification. Ind Crops Prod. 2021;163. DOI: https://doi.org/10.1016/j.indcrop.2021.113329

8. Statista. Statista.com. Leading 10 countries in worldwide beer production in 2020. 2020 [cited 2022 Feb 28]. Available from: https://es.statista.com/estadisticas/1147467/lideres-produccion-cerveza-mundial/

9. Contreras M, Lama-Muñoz A, Romero-García J, García-Vargas M, Romero I, Castro E. Production of renewable products from brewery spent grains. Waste Biorefinery. Elsevier Inc.; 2021. 305–347 p. DOI: http://dx.doi.org/10.1016/B978-0-12-821879-2/00011-9

10. Chetrariu A, Dabija A. Brewer's spent grains: Possibilities of valorization, a review. Applied Sciences. 2020;10(16):1–17. DOI: https://doi.org/10.3390/app10165619

11. Mussatto S, Fernandes M, Rocha G, Órfão J, Teixeira J, Roberto I. Production, characterization and application of activated carbon from Brewer's spent grain lignin. Bioresour Technol. 2010;101(7):2450–7. DOI: http://dx.doi.org/10.1016/j.biortech.2009.11.025

12. Antar M, Lyu D, Nazari M, Shah A, Zhou X, Smith D. Biomass for a sustainable bioeconomy: An overview of world biomass production and utilization. Renewable and Sustainable Energy Reviews. 2021;139:110691. DOI: https://doi.org/10.1016/j.rser.2020.110691

13. Patermann C, Aguilar A. A bioeconomy for the next decade. EFB Bioeconomy Journal. 2021;1:100005. DOI: https://doi.org/10.1016/j.bioeco.2021.100005

14. Brandão A, Gonçalves A, Santos J. Circular bioeconomy strategies: From scientific research to commercially viable products. J Clean Prod. 2021;295. DOI: https://doi.org/10.1016/j.jclepro.2021.126407

15. Hadley E, Hartley S, McLeod C, Polson P. The Sustainable Path to a Circular Bioeconomy. Trends Biotechnol. 2021;39(6):542–5. DOI: https://doi.org/10.1016/j.tibtech.2020.10.015

16. Stegmann P, Londo M, Junginger M. The circular bioeconomy: Its elements and role in European bioeconomy clusters. Resources, Conservation and Recycling: X. 2020;6:100029. DOI: https://doi.org/10.1016/j.rcrx.2019.100029

17. Kao T. Health Potential for Beer Brewing Byproducts. Current Topics on Superfoods. 2018. DOI: https://doi.org/10.5772/intechopen.76126

18. Maqhuzu A, Yoshikawa K, Takahashi F. Prospective utilization of brewers' spent grains (BSG) for energy and food in Africa and its global warming potential. Sustain Prod Consum. 2020;26:146–59. DOI: https://doi.org/10.1016/j.spc.2020.09.022

19. Mallen E, Najdanovic-Visak V. Brewers' spent grains: Drying kinetics and biodiesel production. Bioresour Technol Rep. 2018;1:16–23. DOI: https://linkinghub.elsevier.com/retrieve/pii/S2589014X18300057

20. Rojas-Chamorro J, Cara C, Romero I, Ruiz E, Romero-García J, Mussatto S. Ethanol Production from Brewers' Spent Grain Pretreated by Dilute Phosphoric Acid. Energy and Fuels. 2018;32(4):5226–33. DOI: https://doi.org/10.1021/acs.energyfuels.8b00343

21. Cancelliere R, Carbone K, Pagano M, Cacciotti I, Micheli L. Biochar from Brewers' Spent Grain: A Green and Low-Cost Smart Material to Modify Screen-Printed Electrodes. Biosensors. 2019;9(4):139. DOI: https://www.mdpi.com/2079-6374/9/4/139

22. Gonçalves G, Nakamura P, Furtado D, Veit M. Utilization of brewery residues to produces granular activated carbon and bio-oil. J Clean Prod. 2017;168:908–16. DOI: https://doi.org/10.1016/j.jclepro.2017.09.089

23. Thai S, Avena-Bustillos R, Alves P, Pan J, Osorio-Ruiz A, Miller J. Influence of drying methods on health indicators of brewers spent grain for potential upcycling into food products. Applied Food Research. 2022;2(1):100052. DOI: https://doi.org/10.1016/j.afres.2022.100052

24. Singh A, Mandal R, Shojaei M, Singh A, Kowalczewski P, Ligaj M. Novel drying methods for sustainable upcycling of brewers' spent grains as a plant protein source. Sustainability. 2020;12(9):1–17. DOI: https://doi.org/10.3390/su12093660

25. Mussatto S. Brewer's spent grain: A valuable feedstock for industrial applications. J Sci Food Agric. 2014;94(7):1264–75. DOI: https://doi.org/10.1002/jsfa.6486

26. Kong D, Wang Y, Li M, Liu X, Huang M, Li X. Analysis of drying kinetics, energy and microstructural properties of turnips using a solar drying system. Solar Energy. 2021;230:721–31. DOI: https://doi.org/10.1016/j.solener.2021.10.073

27. Hasibuan R, Sari W, Manurung R, Alexande V. Drying Kinetic Models of Rice Applying Fluidized Bed Dryer. Mathematical Modelling of Engineering Problems. 2023 28;10(1):334–9. DOI: https://doi.org/10.18280/mmep.100138

28. Perazzini H, Perazzini M, Freire F, Freire F, Freire J. Modeling and cost analysis of drying of citrus residues as biomass in rotary dryer for bioenergy. Renew Energy. 2021;175:167–78. DOI: https://doi.org/10.1016/j.renene.2021.04.144

29. Dhurve P, Kumar V, Kumar D, Malakar S. Drying kinetics, mass transfer parameters, and specific energy consumption analysis of watermelon seeds dried using the convective dryer. Mater Today Proc. 2022. DOI: https://doi.org/10.1016/j.matpr.2022.02.008

30. Huang D, Yang P, Tang X, Luo L, Sunden B. Application of infrared radiation in the drying of food products. Trends Food Sci Technol. 2021;110:765–77. DOI: https://doi.org/10.1016/j.tifs.2021.02.039

31. Ertekin C, Firat MZ. A comprehensive review of thin-layer drying models used in agricultural products. Crit Rev Food Sci Nutr. 2017; 57(4):701–17. DOI: https://doi.org/10.1080/10408398.2014.910493

32. Alean J, Maya JC, Chejne F. Mathematical model for the mass transport in multiple porous scales. J Food Eng. 2018;233:28–39. DOI: https://doi.org/10.1016/j.jfoodeng.2018.03.024

33. Chen D, Zheng Y, Zhu X. Determination of effective moisture diffusivity and drying kinetics for poplar sawdust by thermogravimetric analysis under isothermal condition. Bioresour Technol. 2012;107:451–5. DOI: http://dx.doi.org/10.1016/j.biortech.2011.12.032

34. Vega-Gálvez A, Miranda M, Díaz LP, Lopez L, Rodriguez K, di Scala K. Effective moisture diffusivity determination and mathematical modelling of the drying curves of the olive-waste cake. Bioresour Technol. 2010;101(19):7265–70. DOI: https://linkinghub.elsevier.com/retrieve/pii/S0960852410007224

35. Crank J. The mathematics of diffusion. 2nd ed. Oxford university press; 1979.

36. Hall KR, Eagleton LC, Acrivos A, Vermeulen T. Pore- and solid-diffusion kinetics in fixed-bed adsorption under constant-pattern conditions. Industrial and Engineering Chemistry Fundamentals. 1966;5(2):212–23. DOI: https://doi.org/10.1021/i160018a011

37. Arranz JI, Miranda MT, Sepúlveda FJ, Montero I, Rojas CV. Analysis of Drying of Brewers' Spent Grain. Proc West Mark Ed Assoc Conf. 2018;2(23):1467. DOI: https://doi.org/10.3390/proceedings2231467

38. Shroti GK, Saini CS. Development of edible films from protein of brewer's spent grain: Effect of pH and protein concentration on physical, mechanical and barrier properties of films. Applied Food Research. 2022;2(1):100043. DOI: https://doi.org/10.1016/j.afres.2022.100043

39. Medina-Jaramillo C, Quintero-Pimiento C, Díaz-Díaz D, Goyanes S, López-Córdoba A. Improvement of andean blueberries postharvest preservation using carvacrol/alginate-edible coatings. Polymers. 2020;12(10):1–17. DOI: https://doi.org/10.3390/polym12102352

40. Brand-Williams W, Cuvelier ME, Berset C. Use of a free radical method to evaluate antioxidant activity. LWT - Food Science and Technology. 1995;28(1):25–30. DOI: https://doi.org/10.1016/S0023-6438(95)80008-5

41. Ghanem N, Mihoubi D, Bonazzi C, Kechaou N, Boudhrioua N. Drying Characteristics of Lemon By-product (Citrus limon. v. lunari): Effects of Drying Modes on Quality Attributes Kinetics'. Waste Biomass Valorization. 2020;11(1):303–22. DOI: https://doi.org/10.1007/s12649-018-0381-z

42. Bryś A, Kaleta A, Górnicki K, Głowacki S, Tulej W, Bryś J. Some Aspects of the Modelling of Thin-Layer Drying of Sawdust. Energies. 2021;14(3):726. DOI: https://doi.org/10.3390/en14030726

43. Hussain M, Zabiri H, Tufa LD, Yusup S, Ali I. A kinetic study and thermal decomposition characteristics of palm kernel shell using model-fitting and model-free methods. Biofuels. 2022;13(1):105–16. DOI: https://doi.org/10.1080/17597269.2019.1642642

44. Arranz JI, Sepúlveda FJ, Montero I, Romero P, Miranda MT. Feasibility analysis of brewers' spent grain for energy use: Waste and experimental pellets. Applied Sciences. 2021;11(6). DOI: https://doi.org/10.3390/app11062740

45. Sozzi A, Zambon M, Mazza G, Salvatori D. Fluidized bed drying of blackberry wastes: Drying kinetics, particle characterization and nutritional value of the obtained granular solids. Powder Technol. 2021;385:37–49. DOI: https://doi.org/10.1016/j.powtec.2021.02.058

46. Lopez A, Iguaz A, Esnoz A, Virseda P. Thin-layer drying behaviour of vegetable wastes from wholesale market. Drying Technology. 2000;18(4–5):995–1006. DOI: https://doi.org/10.1080/07373930008917749

47. Maia GD, Horta ACL, Felizardo MP. From the conventional to the intermittent biodrying of orange solid waste biomass. Chemical Engineering and Processing - Process Intensification. 2023;188:109361. DOI: https://doi.org/10.1016/j.cep.2023.109361

48. EL-Mesery HS, El-khawaga SE. Drying process on biomass: Evaluation of the drying performance and energy analysis of different dryers. Case Studies in Thermal Engineering. 2022;33:101953. DOI: https://doi.org/10.1016/j.csite.2022.101953

49. Ahmad-Qasem MH, Barrajon-Catalan E, Micol V, Cárcel JA, Garcia-Perez J. Influence of air temperature on drying kinetics and antioxidant potential of olive pomace. J Food Eng. 2013;119(3):516–24. DOI: https://doi.org/10.1016/j.jfoodeng.2013.06.027

50. Şahin Fİ, Acaralı N. Effective moisture diffusivity and activation energy during convective drying of bread containing clove oil/orange oil. Journal of the Indian Chemical Society. 2023;100(3):100952. DOI: https://doi.org/10.1016/j.jics.2023.100952

51. Yan Y, Qi B, Zhang W, Wang X, Mo Q. Investigations into the drying kinetics of biomass in a fluidized bed dryer using electrostatic sensing and digital imaging techniques. Fuel. 2022;308:122000. DOI: https://doi.org/10.1016/j.fuel.2021.122000

52. Lemus-Mondaca R, Zura-Bravo L, Ah-Hen K, Di Scala K. Effect of drying methods on drying kinetics, energy features, thermophysical and microstructural properties of Stevia rebaudiana leaves. J Sci Food Agric. 2021;101(15):6484–95. DOI: https://doi.org/10.1002/jsfa.11320

53. Yan Z, Zhou Z, Jiao Y, Huang J, Yu Z, Zhang D, et al. Hot-Air Drying Significantly Improves the Quality and Functional Activity of Orange Black Tea Compared with Traditional Sunlight Drying. Foods. 2023;12(9):1913. DOI: https://doi.org/10.3390/foods12091913

54. Bai T, Wan Q, Liu X, Ke R, Xie Y, Zhang T. Drying kinetics and attributes of fructus aurantii processed by hot air thin-layer drying at different temperatures. Heliyon. 2023;9(5):e15554. DOI: https://doi.org/10.1016/j.heliyon.2023.e15554

55. Kaveh M, Golpour I, Gonçalves JC, Ghafouri S, Guiné R. Determination of drying kinetics, specific energy consumption, shrinkage, and colour properties of pomegranate arils submitted to microwave and convective drying. Open Agric. 2021;6(1):230–42. DOI: https://doi.org/10.1515/opag-2020-0209

56. Wan Nadhari WNA, Hashim R, Danish M, Sulaiman O, Hiziroglu S. A Model of Drying Kinetics of Acacia mangium Wood at Different Temperatures. Drying Technology. 2014;32(3):361–70. DOI: https://doi.org/10.1080/07373937.2013.829855

57. Nahar N, Hazra S, Raychaudhuri U, Adhikari S. Effect of different drying methods on drying kinetics, modeling, energy-economic, texture profile, color, and antioxidant of lotus rhizomes (Nelumbo nucifera). J Food Process Preserv. 2022;46(10). DOI: https://doi.org/10.1111/jfpp.16842

58. Huang D, Men K, Li D, Wen T, Gong Z, Sunden B. Application of ultrasound technology in the drying of food products. Ultrason Sonochem. 2020;63:104950. DOI: https://doi.org/10.1016/j.ultsonch.2019.104950

Appendix A. Supplementary data

Analysis of drying kinetic of brewer´s spent grains: effect of the temperature on the physical properties and the content of bioactive compounds

Análisis de la cinética de secado del bagazo residual de malta: efecto de la temperatura sobre las propiedades físicas y el contenido de compuestos bioactivo

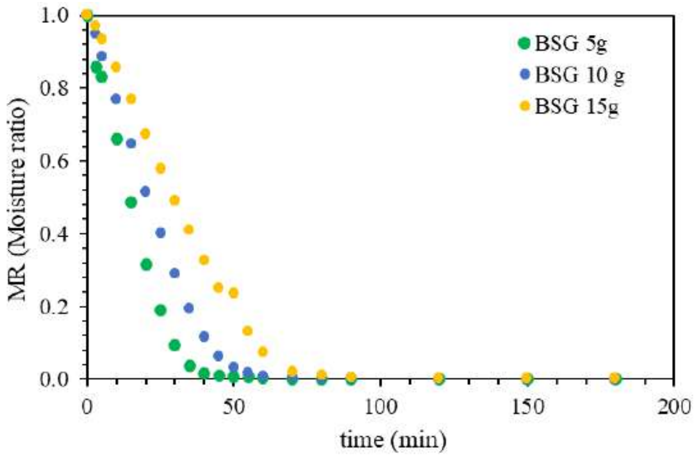

Figure S1. Drying curves at 105°C using different mass of Brewer´s spent grain.

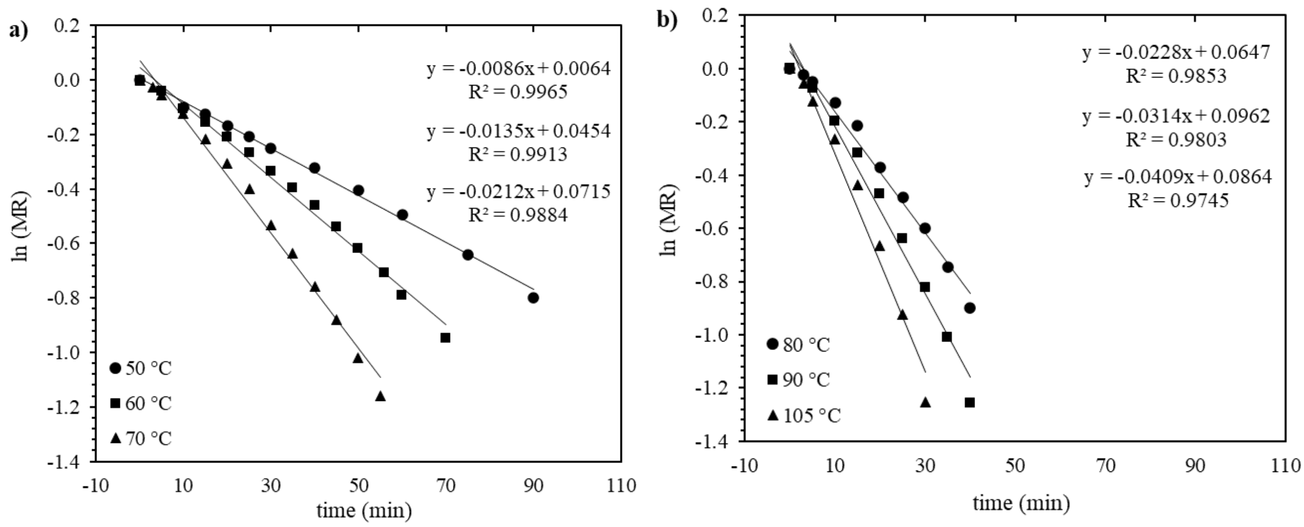

Figure S2. Ln MR vs time, for determination *Deff* at different temperatures 50, 60 y 70 °C a) and 80, 90, 105°C b).

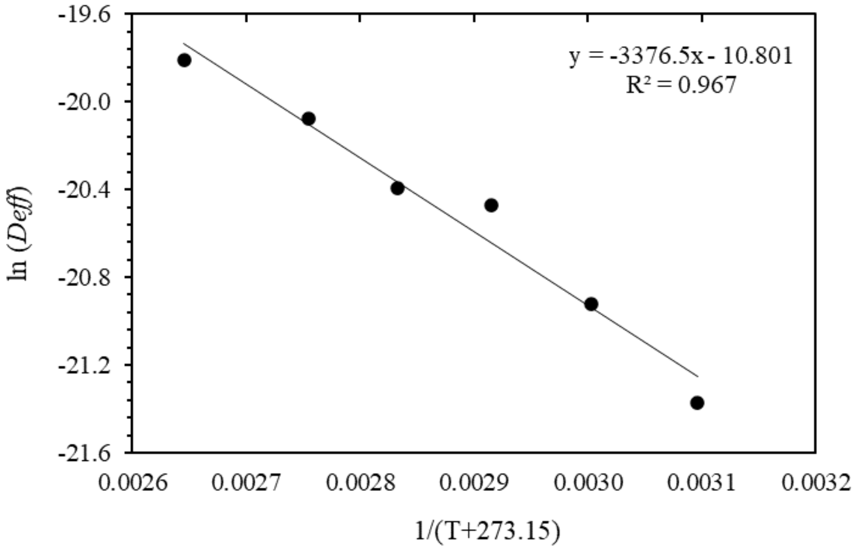

Figure S3. Plot Ln (*Deff*) vs 1/(T+273.15)

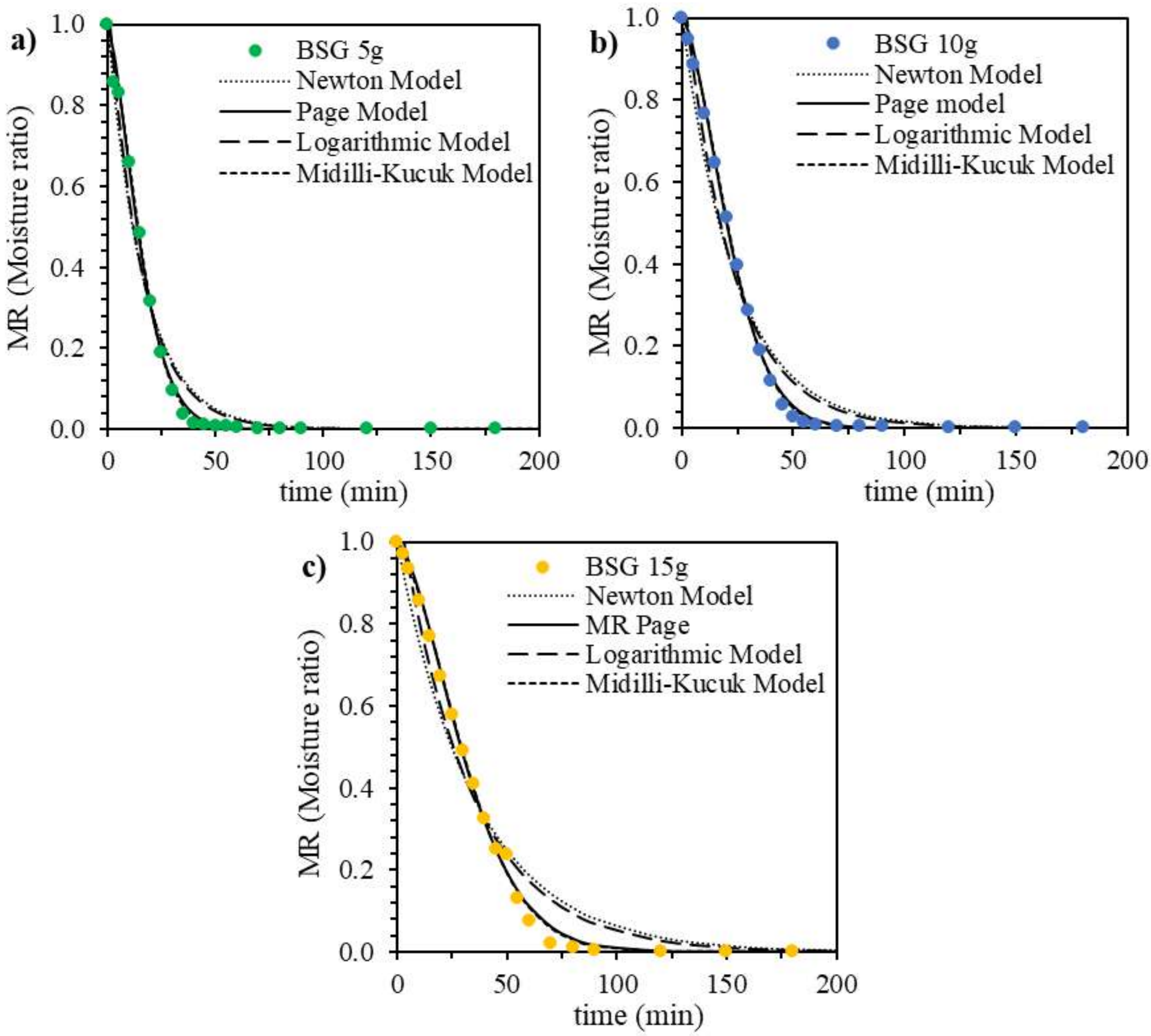

Figure S4. Kinetic models to describe the drying process using different masses of BSG to dry: 5g (a), 10 (b) and 15g (c). Drying temperature: 105 °C.

Table S1. Parameters of the different drying kinetic models using different BSG mass at constant temperature of 105°C.

Modelo	Sample mass	Parameters				Statistics		
	(g)	a	b	n	K (s^n)	r^2	*SD*	*CV*
Newton	5	-	-	-	0.0600	0.9748	0.053	0.233
	10	-	-	-	0.0420	0.9647	0.065	0.222
	15	-	-	-	0.0279	0.9585	0.073	0.189
Page	5	-	-	1.4564	0.0153	0.9956	0.021	0.094
	10	-	-	1.5728	0.0063	0.9975	0.017	0.057
	15	-	-	1.5805	0.0034	0.9968	0.020	0.051
Logarítmico	5	5.00E-06	1.0693	-	0.0639	0.9767	0.048	0.211
	10	5.00E-08	1.0968	-	0.0458	0.9700	0.056	0.190
	15	8.00E-08	1.1000	-	0.0308	0.9670	0.062	0.159
Midilli-Kucuk	5	0.9548	9.21E-06	1.6085	0.0092	0.9966	0.018	0.078
	10	0.9711	5.00E-07	1.6678	0.0044	0.9979	0.014	0.048
	15	0.9795	6.00E-08	1.6464	0.0026	0.9969	0.018	0.047

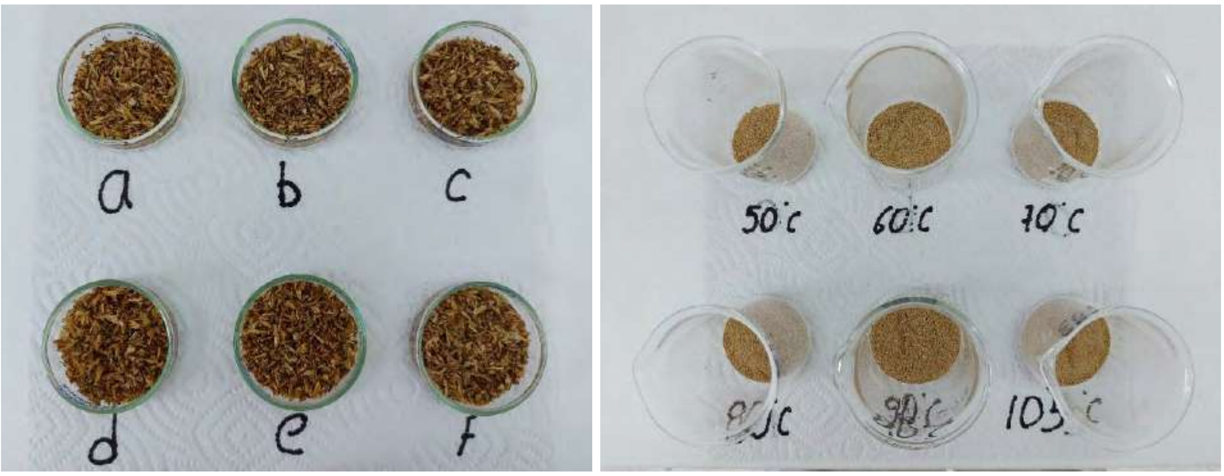

Figure S5. Brewer´s spent grain (BSG), BSG dry and entire (left) and BSG dry and ground (right).

Table S2. Drying kinetic models parameters, at a constant temperature of 105°C.

Temperature (°C)	Whole BSG				Ground BSG			
	L	a+	b-	ΔE	L	a+	b-	ΔE
50	31.8	8.7	26.5	58.10	53.9	4.8	17.5	34.30
60	32.1	6.5	24.1	56.36	50.2	5.2	16.8	37.04
70	33.9	10.5	24.2	55.54	51.8	2.5	19.7	36.95
80	32.5	9.8	24.7	56.84	52.6	4.7	17.2	35.17
90	34.1	9.1	22.9	54.48	53.1	3.9	18.5	35.37
105	33.5	10.2	23.9	55.68	54.2	5.2	18.1	34.48